doi:10.1016/j.jmb.2005.08.065 J. Mol. Biol. (2005) 353, 772–787

JMB

Available online at www.sciencedirect.com

SCIENCE DIRECT®

ELSEVIER

Effects of Donor and Acceptor RNA Structures on the Mechanism of Strand Transfer by HIV-1 Reverse Transcriptase

Mark Nils Hanson[1], Mini Balakrishnan[1], Bernard P. Roques[2] and Robert A. Bambara[1,3]*

[1]*Department of Biochemistry and Biophysics, University of Rochester Medical Center Rochester, NY 14642, USA*

[2]*Departement de Pharmacochimie Moleculaire et Structurale, U266 INSERM URA D1500 CNRS, UER des Sciences Pharmaceutiques et Biologiques, 4 Avenue de l'Observatoire, 75270 Paris Cedex 06, France*

[3]*Cancer Center, University of Rochester Medical Center Rochester, NY 14642, USA*

**Corresponding author*

Template switching during reverse transcription contributes to recombination in human immunodeficiency virus type 1 (HIV-1). Our recent studies suggest that the process can occur through a multi-step mechanism involving RNase H cleavage, acceptor invasion, branch migration, and finally primer terminus transfer. In this study, we analyzed the effects of reverse transcriptase (RT)-pausing, RNase H cleavages and template structure on the transfer process. We designed a series of donor and acceptor template pairs with either minimal pause sites or with pause sites at various locations along the template. Restriction sites within the region of homology allowed efficient mapping of the location of primer terminus transfer. Blocking oligomers were used to probe the acceptor invasion site. Introduction of strong pause sites in the donor increased transfer efficiency. However, the new pauses were not necessarily associated with effective invasion. In this system, the primary invasion occurred at a region of donor cleavage associated with weak pausing. These results together with acceptor structure predictions indicated that a potential invasion site is used only in conjunction with a favorable acceptor structure. Stabilizing acceptor structure at the predicted invasion region lowered the transfer efficiency, supporting this conclusion. Differing from previous studies, terminus transfer occurred at a short distance from the invasion site. Introduction of structure into the acceptor template shifted the location of terminus transfer. Nucleocapsid protein, which can improve cDNA–acceptor interactions, increased transfer efficiency with some shift of terminus transfer closer to the invasion site. Overall results support that the acceptor structure has a major influence on the efficiency and position of the invasion and terminus transfer steps.

Keywords: HIV-1; reverse transcriptase; strand transfer; RNA structure; template switching

Introduction

The genome of HIV-1 is packaged as two plus-strand RNAs. These are reverse transcribed by the virally encoded reverse transcriptase (RT) to form double-stranded DNA, which is integrated into the host genome.[1,2] Viral replication requires two strand transfer events at the ends of the template, minus strand strong stop transfer, and plus strand transfer.[3] Along with these obligatory end transfers, strand transfer has also been demonstrated to occur within internal regions of the genome.[4–6] Strand transfer occurs when the elongating cDNA stops copying one template, the donor, and continues on another homologous template, the acceptor.

HIV-1 is one of the most recombinogenic retroviruses, having as many as three crossovers occurring per genome per replication cycle,[7,8] with

Present address: R. A. Bambara, Department of Biochemistry and Biophysics, Box 712, University of Rochester Medical Center, 601 Elmwood Ave, Rochester NY 14642, USA.

Abbreviations used: HIV-1, human immunodeficiency virus type 1; RT, reverse transcriptase; NC, nucleocapsid protein; *TE*, transfer efficiency.

E-mail address of the corresponding author: robert_bambara@urmc.rochester.edu

markers only 1 kb apart showing nearly random segregation.[9] Consequences of recombination include helping the virus evade the host immune system by genomic shuffling,[10,11] combining drug-resistant mutations,[12–14] and dispersing mutations introduced by the low-fidelity RT.[15–19]

Recombination can occur during both plus and minus strand synthesis. However, studies have shown that it occurs primarily during minus strand synthesis.[7,20–22] Minus strand transfer was described as occurring by a copy choice mechanism,[23] and is dependent on both the RNase H activity of RT,[24–31] and template homology.[32–37] In this mechanism the extending cDNA primer transfers from the initial template, or donor, to another RNA template, or acceptor.

While several templates with little or no pausing have recently been shown to support transfer quite efficiently,[38–40] pausing has been demonstrated to facilitate transfer.[27,41–47]

Pause-initiated transfers appear to occur by a multi-step mechanism.[38,41,46,48–50] Pause sites produce multiple RNase H cleavages that are closely spaced, leading to clearing of the donor RNA from the cDNA.[41,46] Clearing creates a potential site for the acceptor to interact with the cDNA. This interaction has been described as an invasion.[50,51] The acceptor invasion is the first contact between the cDNA and acceptor. As the RT resumes synthesis on the donor, this interaction propagates by branch migration. Transfer is completed with the capture of the primer terminus by the acceptor, which occurs at a position removed from the initial invasion site. The distance between invasion and terminus transfer varied in different template systems.

Nucleocapsid protein (NC) is an RNA chaperone that aids in the formation of the most thermodynamically stable conformation.[52,53] NC also has an important role in increasing the efficiency of transfer.[54–56] NC is thought to accomplish this by assisting in annealing two nucleic acid strands.[48,57–62] Several groups have suggested that NC specifically aids in the interaction of the acceptor with the cDNA, increasing invasion.[39,41,49,63–65] Another transfer-promoting function of NC is its ability to increase RT RNase H activity, leading to an increased concentration of significant cleavages at strong pause sites.[41,46,66]

Here, we set out to determine the role of pause sites and secondary structure of the donor and acceptor RNA templates on the mechanism of strand transfer. The results showed that increased cleavage of the donor at a strong pause site did not always create an effective invasion site. Additionally we found that structures in the acceptor influence its ability to interact at a potential invasion site, and effect the location of primer terminus transfer.

Results

Our previous analysis of HIV-1 RT-promoted transfers using various RNA templates *in vitro* indicated a separation of the acceptor invasion and terminus transfer steps.[38,41,50] To better understand the role of pausing and RNA template characteristics that promote transfer, we designed a template system in which sequences could be manipulated to

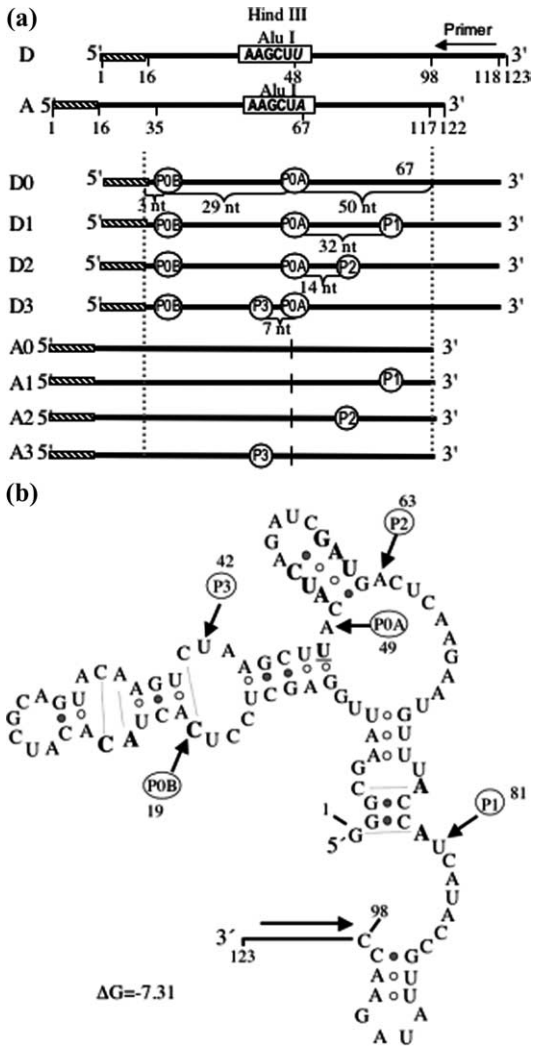

Figure 1. Diagram of the RNA templates. (a) Donor and acceptor templates, the marker which is a single nucleotide change between the templates (italics), removes a HindIII recognition sequence from the acceptor template. Hatched regions on the donor and acceptor represent the plasmid-derived sequence. Synthesis is initiated by primer binding to the unique sequence at the 3′ end of the donor templates (black arrow). The acceptor shares 82 nt of homology with the donor, and has a 19 nt extension 5′ of the region of homology allowing for separation of full-length extension and transfer products. A schematic showing the four donor and four acceptor templates used is included. The locations of pause sites on the templates are labeled P0A through P3, and the pertinent distances are shown. (b) One of the Mfold-predicted structures of D0. Bases mutated to strengthen structures are shown in bold and new interactions created are shown with broken lines. Locations of pause sites on D0 and introduced on the templates that include these mutations are shown.

alter the secondary structure, influencing RT pausing at various locations on the template. Sites of transfer initiation and completion could then be correlated with specific structural features.

Design of the templates

The transfer system consists of a 123 nt donor RNA and a 122 nt acceptor RNA that share an internal 82 nt region of homology (Figure 1(a)). The donor template has a unique primer-binding site at its 3′ end. A short non-homologous region following the region of homology on the acceptor prevents end transfers. In this way, the system simulates internal recombination events. The donor and acceptor templates have an AluI cleavage site about 50 nt from the primer binding site. We introduced a single nucleotide substitution at position 48 in the donor template to create a HindIII cleavage site, overlapping with the AluI site. This enabled efficient mapping of the location of primer terminus transfer by restriction digestion of the transfer products.

The initial donor and acceptor templates, D0 and A0, were designed such that they lacked strong secondary structures with the anticipation that they would promote minimal RT-pausing during synthesis. Figure 1(b) shows one of the secondary structures of D0 as predicted by Mfold.[67] Primer extension assays on this donor revealed several weak pause sites (Figures 2 and 3). P0A at position 70 decreases with time while P0B, at position 100, is relatively constant throughout the time-course (Figure 3). A series of weak pause sites were also observed in the 20–40 nt and 45–55 nt regions (Figures 2 and 3).

We generated three additional donor templates from D0, by strengthening existing weak secondary structures at different locations within the region of homology (Figure 1). This was accomplished by introducing minimal sequence substitutions into D0 (see Materials and Methods). The intention was to create a series of donor templates, D1, D2 and D3 (Figure 1), each with unique pause sites at distinct locations within the region of homology. A similar approach was used to generate the structured acceptors A1, A2 and A3 from the initial acceptor A0 (Figure 1). In order to determine whether the sequence modifications introduced were effective in creating stable structures on the templates, we performed primer extensions on the donor and acceptor templates (Figure 2). Each of the new donors displayed unique pause sites at the expected locations, which we will refer to as P1, P2, and P3 (Figure 2). Acceptor templates were extended with a primer that was shifted 17 nt into the region of homology. Each acceptor had the same strong pause sites (P1, P2, and, P3) as the corresponding donor template. All four acceptors also shared the pause site, PA, within the non-homologous region (Figure 2). The pause sites, P1, P2, and P3, in the donor and acceptor templates confirm the presence and location of prominent secondary structure in the templates. Further, these results demonstrate that our approach of stabilizing structures in the RNA templates, based on Mfold secondary structure predictions was successful in generating the expected RT pause sites in the donor and acceptor pairs.

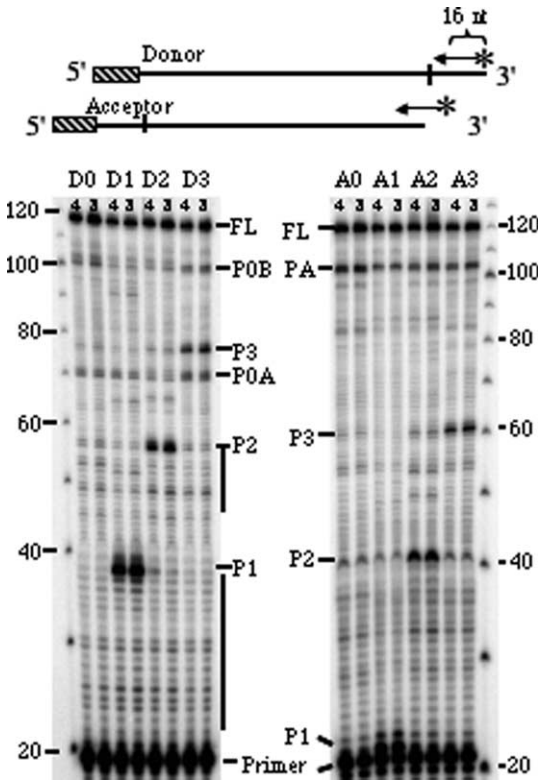

Figure 2. Primer extension on donor and acceptor templates. The (5′-^{32}P) end-labeled MH21 and MH65 primers, used with the donor and acceptor templates respectively, were used for extension assays as shown. Extension products were 16 nt longer on the donor than on the acceptor templates. Reactions were stopped after 4 min and 8 min, and separated on an 8% polyacrylamide gel. The primer, pause sites on the donor and acceptor templates (P0A, POB, P1, P2, P3), full-length donor and acceptor products (FL), and a pause site unique to the acceptor templates (PA) are labeled. A series of weak pause sites (20–40 nt and 45–55 nt) present in all the donors are labeled by vertical bars to the right of the panel. Size standards are labeled on the outside of each panel.

Effect of pausing on transfer

To assess the effects of the presence and location of pause sites on template switching, we performed transfer assays with the various donor and acceptor template pairs. Transfers were first analyzed using each of the donors in combination with the less structured acceptor, A0 (Figure 3). Full-length donor extension products (FL) were 118 nt long. When the primer switched from the donor to the acceptor template full extension produced a 137 nt

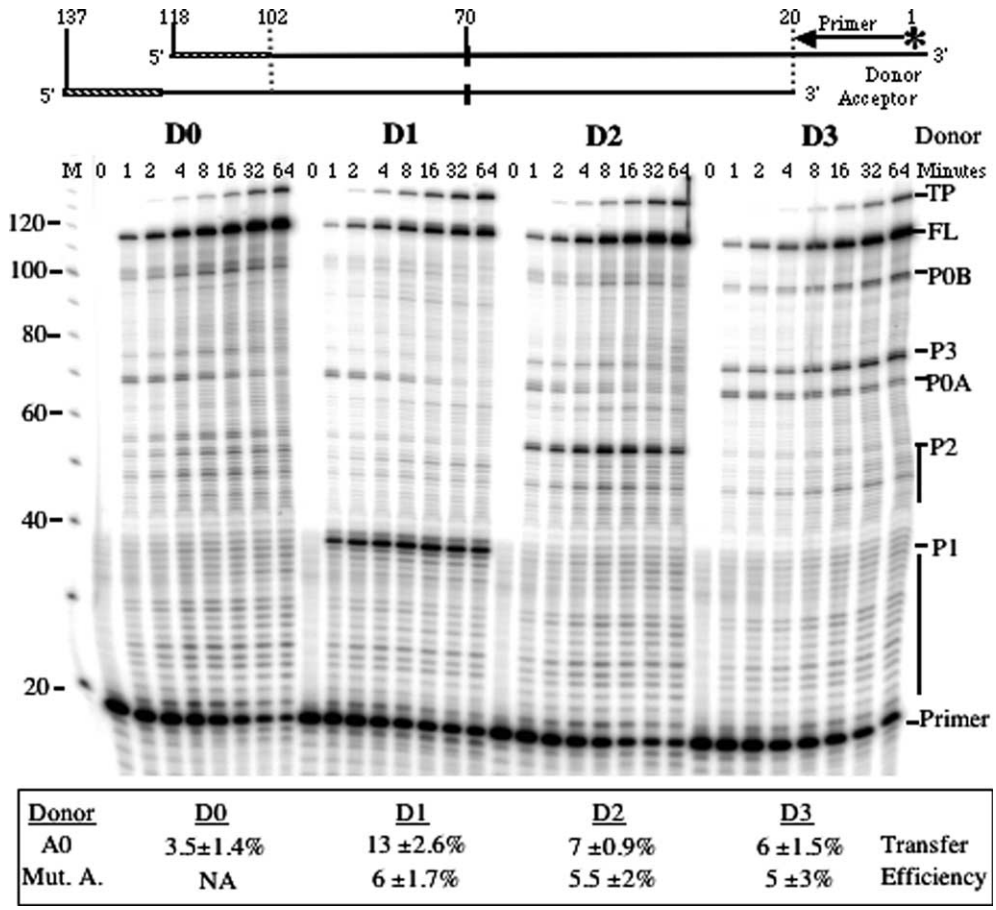

Figure 3. Time-course of transfer reactions. The (5′-^{32}P) end-labeled MH21 primer was annealed to the various donor templates and extension reactions were performed as shown, in the presence of twice as much initial acceptor (A0). Products were sampled at increasing times (0, 1, 2, 4, 8, 16, 32 and 64 min), and separated on an 8% polyacrylamide gel. Products seen during extension from the bottom are the primer, various pause sites in each template (P0A, POB, P1, P2, P3), the full-length donor extension product (FL), and the transfer product (TP) which are labeled on the right of the panel. A series of weak pause sites (20–40 nt and 45–55 nt) present in all the donors are labeled by vertical bars. Size standards are labeled on the left. The transfer efficiency of each donor template with both A0 and the corresponding mutant acceptor (Mut. A) after 30 min is given below the gel. Results represent the average of at least three experiments.

transfer product (TP). Transfer efficiency (*TE*) was calculated as $TE = \mathrm{TP}/(\mathrm{TP} + \mathrm{FL}) \times 100$, and was determined with each donor template and A0 (Figure 3). The *TE* value of the donor templates with additional pause sites (D1, D2, and D3) was two to four times that of the less structured D0 (Figure 3). D1 gave the highest *TE* value of 13(±2.6)%, while D0 yielded only 3.5(±1.4)%.

Pausing on the donor increased local RNase H cleavage

Suo & Johnson have shown that pausing of polymerization at template structures does not alter the rate of RNase H activity[68,69] but has the effect of concentrating RNase H cleavages. Consistent with this, RT pausing has been shown to increase RNase H cleavages immediately 3′ to pause sites on the RNA.[41,46,70] Such localized cleavages can create an effective invasion site for transfer. To examine the pause-associated RNase H cleavages within the modified templates, we followed degradation of the donor RNA template during the course of the transfer reaction (Figure 4). Donor RNAs were labeled at the 5′ end.

D0 showed three regions of cleavages: a series of closely spaced cleavages at the template 3′ end (100–120 nt region), corresponding to the region of primer annealing, and located outside the region of homology, a series of cuts towards the 3′ region of homology (58–98 nt region), and cuts towards the template 5′ end (15–40 nt). Analysis of the cleavage products in correlation with the pause sites indicated that cleavages in the 58–98 nt region are very likely associated with the P0A pause site and the weak pause sites between 45 nt and 55 nt. The 28 nt and 38 nt cuts very likely result from the P0B pause site. Each of the modified donors also had increased RNase H cleavages 3′ of the introduced pause site. This was inferred from the increased intensity of bands at early time-points, before these cleavages could be masked by cleavages associated with progression of polymerization to the 5′ end of the templates. For the D1 donor, the P1 pause site

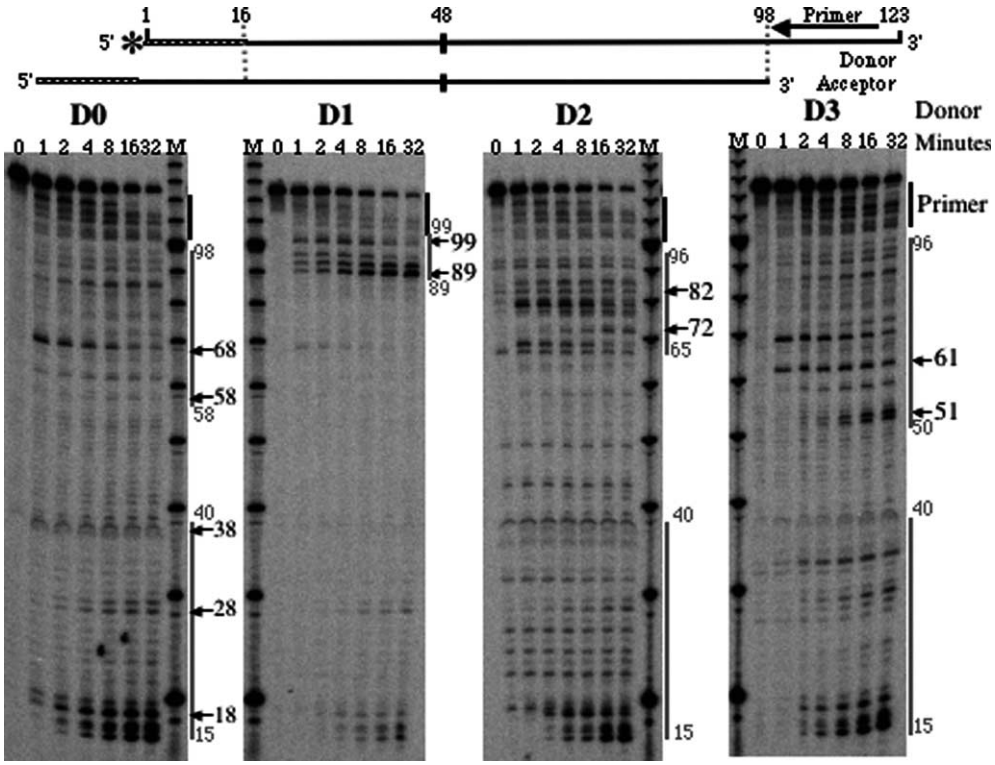

Figure 4. RNase H cleavage profile during extension. Donor RNA with a (5′-^{32}P) end label was followed during primer extension reactions performed as described for Figure 3. Reactions were sampled after (0, 1, 2, 4, 8, 16, and 32 min) from left to right, and separated on a 10% polyacrylamide gel. The region covered by primer MH21 is labeled with a bar beside each panel. Cleavages that occur on all four templates are labeled to the right of the first panel (D0). Cleavages on each template that correspond to the introduced pause site are labeled on the right of each panel. Grey bars represent regions of cleavage on each template. A ten base-pair ladder is included in each (lane M).

noticeably stalled synthesis, resulting in fewer primers completing synthesis to the end of the template (Figure 3). The rapid accumulation of cleavage products between 89 nt and 99 nt, and the small amount of terminal cleavage products (Figure 4, D1) support this observation. In the case of D2, an additional series of cuts were observed in the 65–96 nt region when compared to D0, resulting from P0A and the newly introduced pause site P2. Finally, for D3, additional prominent cleavage products were observed in the 50–98 nt region, and are predicted to result from pause-associated cleavage from P0A, P3, and the weak pause sites between 45 nt and 55 nt. Along with these additional cleavages both D2 and D3 had a series of cleavages at the 3′ (100–120 nt) and 5′ (15–40 nt) ends of the template similar to D0. Key observations from the RNase H analysis were: (1) introduced pause sites correlated with increased RNase H cuts in each of the modified donors; (2) several weak pause sites were effective at promoting efficient RNase H cleavage of the templates.

Determination of invasion sites using blocking oligonucleotides

We predicted that increased RNase H cleavage corresponding to the newly introduced pause sites on these templates would stimulate the acceptor invasion step of strand transfer at such sites. We previously developed a method in which short oligonucleotides complementary to various regions of the cDNA were used to interfere with acceptor–cDNA interactions, and thereby inhibit transfer.[38,41,46] An inhibition of transfer by a blocking oligomer is taken as an indication of cDNA–acceptor interaction at that site during transfer. A series of oligonucleotides between 18 nt and 30 nt in length were designed, representing specific sections of donor–acceptor homology (Figure 5(a)). The sequence of the DNA oligomers was the same as the template. A control having the G oligomer sequence in the reverse orientation was shown to have no effect on any of the template pairs (Figure 5(b)–(e)).

We first analyzed the effect of the blocking oligomers on transfers to the unstructured acceptor, A0 (Figure 5(b)). For D0, oligomers B and D, which correspond to the region of extensive cleavage at the donor 3′ region (Figure 4; 58–98 nt region), inhibited transfer by 51.4(±7)% and 37.3(±9.5)%, respectively. This suggests that acceptor–cDNA interactions that facilitate transfer are promoted in this region. Interestingly, oligomer G, which covers the region of homology at the 5′ end, also inhibited transfers by 47.3(±5)%. For donor D1, the P1 pause site promoted RNase H cleavages in the region of oligomer B. For this donor, although oligomer B as

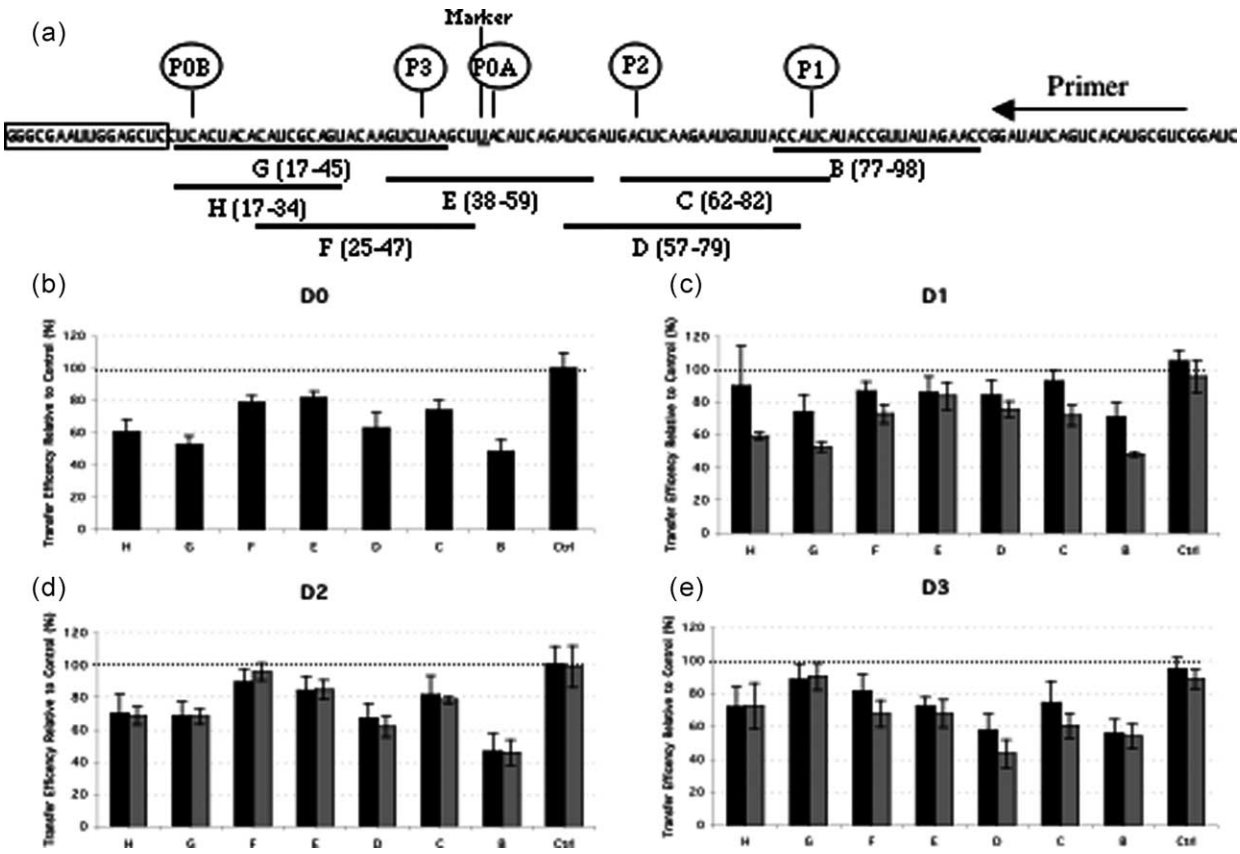

Figure 5. Effect of blocking oligonucleotides on strand transfer. (a) The sequence of D0 is shown. The location of pause sites introduced on the various donor templates is labeled. Blocking oligonucleotides are aligned opposite their homologous region of the donor template. The box represents the plasmid-derived sequence. ((b)–(e)) Quantification of transfer reactions performed with each donor and A0 (black bars), or the acceptor with the corresponding mutations (gray bars), in the presence of blocking oligonucleotides. The transfer efficiency in the absence of blocking oligonucleotides was set as 100%. The relative transfer efficiency with each blocking oligonucleotide is plotted. The Ctrl oligomer has the same sequence as G in reverse orientation. Results represent the average of at least four experiments.

expected was most effective at inhibiting transfer, the inhibition was only 29(±8.5)%. Oligomer G caused a similar inhibition, decreasing transfers by 26(±11)%. For donor D2, which had increased RNase H cleavage in the 65–96 nt region, we anticipated oligomers B, C and D to be equally effective. Here again, oligomer B was the most effective and inhibited transfers by 53.5(±11)%, while oligomer D caused a 32.8(±9)% inhibition. Both oligomers G and H, corresponding to the template 5′ end also inhibited transfers by 31.5(±9)%. Finally, in the case of D3, which had extensive RNase H cleavages in the region covered by oligomer D (57–79 nt), both oligomers B and D were the most inhibitory to transfer (40–45% inhibition). In summary, for each of the four donors, oligomer B was found to be most inhibitory to transfers. We considered this to indicate that the 77–98 nt region of the donor is a potential site of acceptor–cDNA interaction, and is very likely involved in transfer. This remained true even after the introduction of pause sites that increased RNase H cleavage producing a potential invasion site elsewhere. These data implicate factors in addition to donor cleavage as influencing acceptor invasion.

Influence of acceptor structure on invasion

To address whether acceptor structure affects transfer we generated acceptors with similar sequence and structural features as the donor. For the donors D2 and D3, changing the acceptor template from A0 to the corresponding structured acceptors A2 or A3, had minimal effect on *TE* (Figure 3). However, for donor D1, the change from A0 to A1 reduced the *TE* by half (Figure 3). A likely interpretation for the reduced transfer is that the stabilized structure in A1 interferes with invasion, thereby impeding transfer.

We next analyzed the effect of the blocking oligomers on transfers involving the structured acceptor templates. For each of the three structured donors, D1, D2, and D3, the overall profile of transfer inhibition by the various blocking oligomers remained the same with A0 and their corresponding structured acceptor, with oligomer B being the most effective (Figure 5(c)–(e); gray

bars). This indicates for these templates that the primary site available for invasion within the donor–cDNA hybrid remained the same irrespective of the acceptor template. In the case of donor D1, the blocking oligomers, in general, were more effective at inhibiting transfers with acceptor A1 as compared to A0 (Figure 5(b)). Likely, a stabilized structure in this acceptor made invasion less efficient, allowing the blocking oligomers to compete more effectively with the acceptor and inhibit transfer.

Determining structure of A0 and A1 by RNase T_1 digestion

To address how acceptor structure might affect the invasion site and transfer we performed structure predictions using Mfold.[67] Predictions indicated that A0, A2, and A3 all had similar structures in the putative invasion site (data not shown), defined by donor cleavage (Figure 4), and blocking oligomer B (Figure 5). Consistent with this, A2 and A3 did not alter the transfer efficiency significantly compared to A0 (Figure 3), nor alter the effect of the blocking oligomers (Figure 5(d) and (e); gray *versus* black bars). In contrast, A1 caused a significant decrease in *TE*. Therefore, we focused on comparing the structure of the A0 and A1 templates.

When RNase T_1 digestion was performed (Figure 6(a)), and used to constrain Mfold the predicted structures of A0 and A1 showed noticeable differences, particularly in the predicted region of invasion covered by oligomer B, the 96–117 nt region of the acceptors (compare Figure 6(b) and (c)). In the case of A0, this region is weakly structured with only two G-C base-pairs, consistent with its ability to utilize this region efficiently for invasion. The same region in A1, on the other hand, includes seven G-C base-pairs, creating a much more stable structure that is less likely to be in an open conformation able to interact efficiently with the cDNA. This difference in structural stability of the two acceptor templates can explain why A1 decreases the transfer efficiency of D1, compared to A0.

If this interpretation were true, then use of acceptor A1 in place of A0 should reduce the

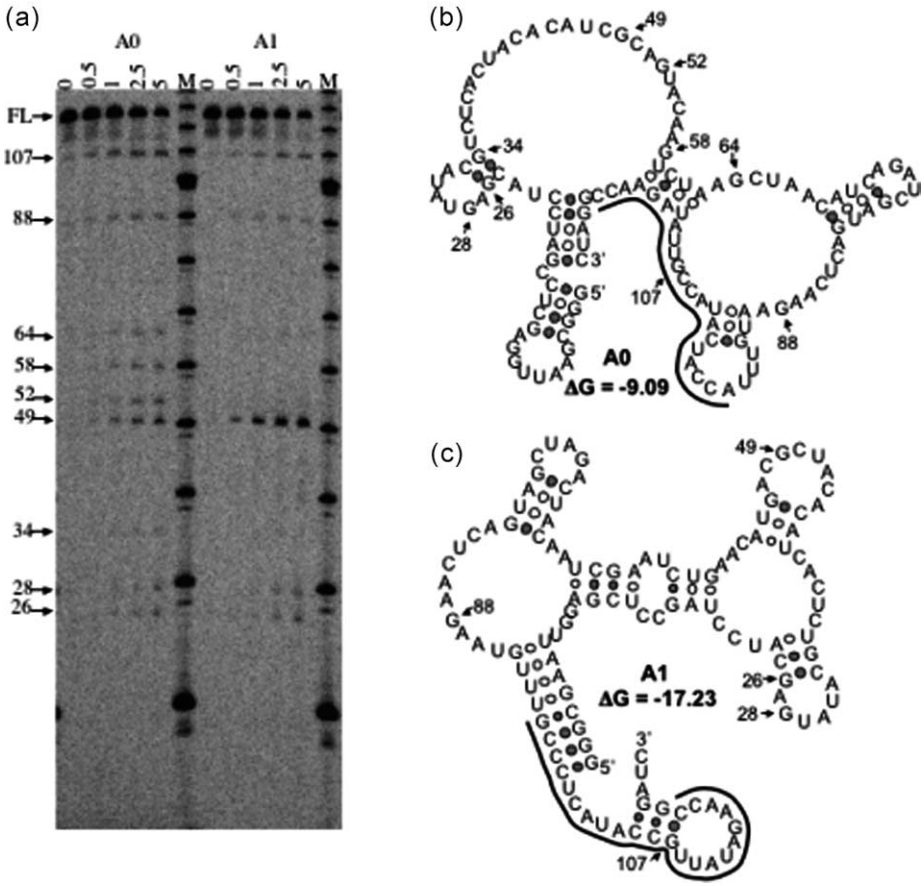

Figure 6. RNase T_1 digestion and structural modeling of A0 and A1. (a) (5′- ^{32}P) end-labeled A0 or A1 templates were incubated with RNase T_1 and the reactions were sampled at increasing time (0, 0.5, 1, 2.5, and 5 min) from left to right, and separated on a 10% polyacrylamide gel. The cleavage bands are labeled on the left according to their respective position within the template sequence. A 10 bp DNA ladder was included as a reference (lane M). (b) and (c) Structures predicted by Mfold constrained by the RNase T_1 digestion data in (a) for A0 and A1, respectively. The residues cleaved by RNase T_1 are numbered, and the region corresponding to blocking oligomer B is marked by a line.

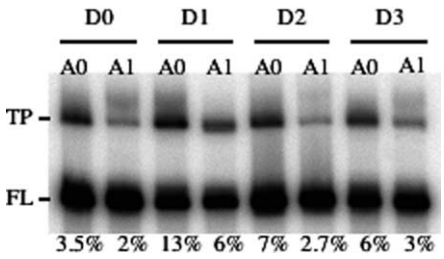

Figure 7. The transfer efficiency with A0 and A1 on all four donors. Transfer reactions were performed for 30 min as described for Figure 3 using each donor with either A0 or A1. The full-length donor extension product (FL) and transfer product (TP) are labeled to the left. The transfer efficiency of each donor–acceptor pair after 30 min is given below the gel. Results represent the average of at least three experiments.

transfer efficiency for the remaining three donors as well, since the 57–98 nt region is predicted to be a primary acceptor–cDNA interaction site for all four of the donor templates. A1 was found to decrease the transfer efficiency by approximately half for all of the donors (Figure 7). These data suggest that creation of an effective invasion site requires a favorable combination of donor cleavages and acceptor structure.

Analysis of the primer terminus transfer site

Previous analysis of transfers in a variety of templates revealed that the primer terminus switch occurred at a site removed from the predicted invasion site.[38,41,46] To determine the location of the primer terminus transfer in transfer products generated in the present system, we isolated the transfer products, amplified by PCR and digested using HindIII (Figure 8(a)) (see Materials and Methods for details). Only the transfer products that result from primer terminus switch after copying template nucleotide number 48 from the donor, will be cleavable by HindIII. Therefore, the percentage cleaved by HindIII is indicative of the percentage of transfers that result from primer terminus switch after the marker nucleotide. AluI, whose 4 nt recognition sequence is central to the 6 nt HindIII recognition sequence, was used as an internal control to determine the amount of cleavable product. Total cleavable product varied between 92% and 98% (Figure 8).

We first analyzed transfer products generated by each of the four different donor templates when used with the less structured acceptor, A0 (Figure 8(b)). With donor D0, almost half the terminus transfers were completed within the first 50 nt of homology (before the marker), while slightly over 50% transferred within the last 30 nt of homology. For D1 and D2, about 85% of terminus transfers occurred before the marker, i.e. within the first 50 nt of homology and in close proximity to the invasion site. In the case of D3, about 60% of the transfers occurred before the marker. Control reactions to determine how much recombination could occur during PCR amplification were performed as follows. Equal amounts of donor and acceptor extension products were extracted from a gel and PCR-amplified using either two external primers, which could only produce a full-length product by recombination, or two internal primers that could amplify both the donor and acceptor templates (Figure 8(a)). The percentage of radioactivity in each lane representing full-length product was determined, and the ratio between the two primer sets defined a maximum recombination rate of less than 1% from the PCR amplification (Figure 8(a)). These results indicate that amplification errors could not alter the relative amounts of each restriction site significantly.

Effect of NC on transfers

Nucleocapsid protein NC, which increases RNase H activity and promotes strand annealing, has been demonstrated to increase strand transfer.[38,46,60,61,66,71,72] Transfer reactions were performed with increasing amounts of NC, and a 50% NC coating was found to be optimal (data not shown). NC increased the overall transfer efficiency for each template pair to about five times, although the relative transfer efficiencies between the various templates was unchanged (compare Figure 8(b) and (c)).

Analysis of transfer distribution showed that NC had only a modest effect on the distribution of transfers (Figure 8(c)). For D0 and D3, transfers before the marker increased from 46(±8)% to 62(±4)% and from 58(±4)% to 68(±)5%, respectively (compare Figure 8(b) with (c)). The strand exchange properties of NC very likely enhanced propagation of the invasion hybrid toward the primer terminus, decreasing the distance between the transfer steps. For donors D1 and D2, where transfers predominantly occurred before the marker, NC did not cause any significant change in the distribution of primer terminus transfer.

Structured acceptor templates can shift transfer distribution

To further address the role of acceptor structure on transfer, we compared the distribution of transfer products formed with the less-structured acceptor A0, or the structured acceptors. With donor D1, acceptor A1, which caused a significant drop in the transfer efficiency, also altered the distribution of transfers, increasing the percentage of transfers after the marker from 16(±4.5)% to 30(±6)% (compare Figure 8(b) and (d)). In the case of D3, changing acceptor from A0 to A3 did not alter transfer efficiency; however, transfers after the marker increased from 42(±4)% to 59(±7)%. In contrast, A2 had no effect on the transfer properties of D2, with the transfer efficiency, region of

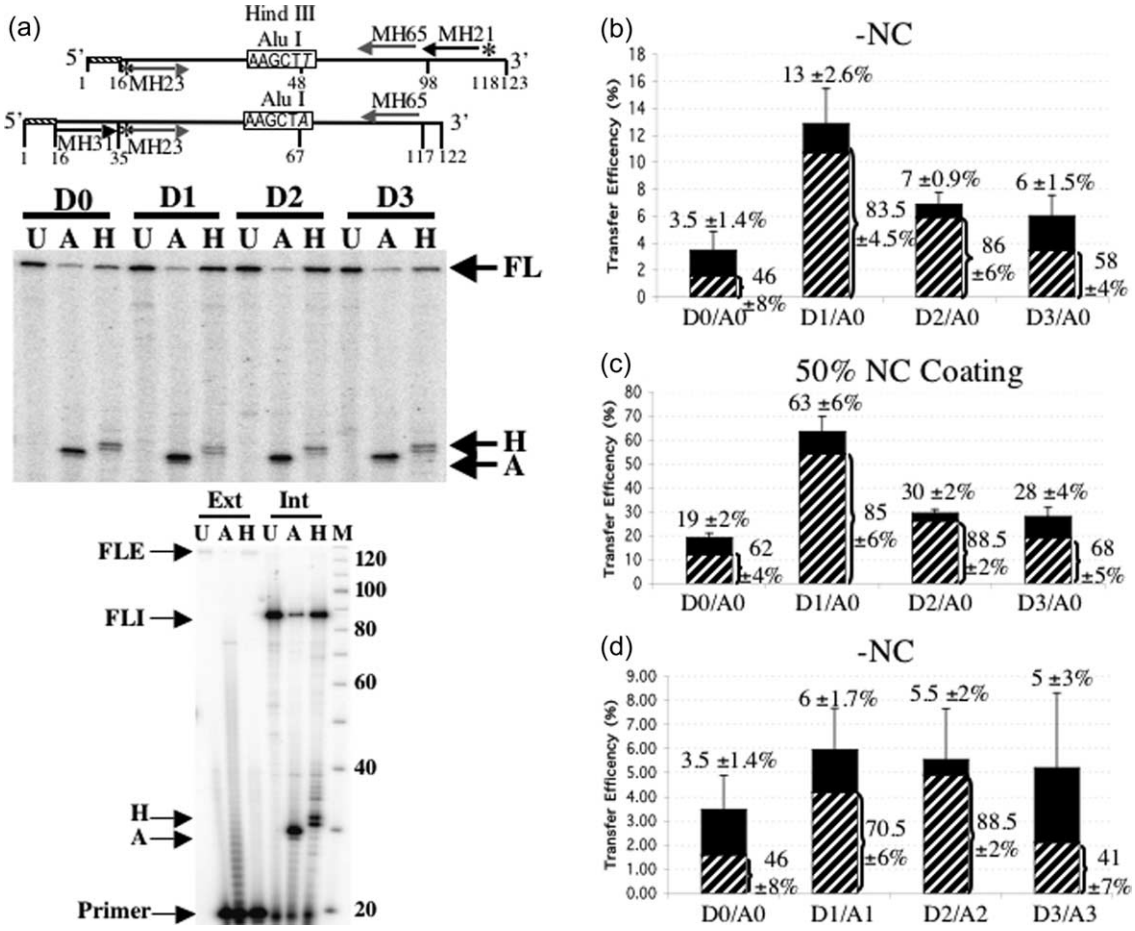

Figure 8. Transfer efficiency and distribution of primer terminus transfer. (a) Transfer products were extracted from the gel and PCR amplified using the external primer set MH31 and 5′ end-labeled MH21. PCR products were undigested (U), or digested with HindIII (H), which can only cleave products that transferred after the marker, or digested with AluI (A), which cleaves all transfer products, and separated on a 10% polyacrylamide gel. Full-length PCR product (FL) and the bands from either HindIII (H) or AluI (A) are labeled on the right. Control reactions using equal amounts of donor and acceptor extension products are shown in the bottom panel. Reactions were performed using either the external primer set (Ext) shown in black, which produced a recombinant full length product (FLE), or the internal primer set (Int) MH23 and MH65 shown in gray, which produced a full length product (FLI). AluI and HindIII digestion products and the unused primer are also labeled to the left of the panel. A 10 bp ladder (M) was included and bands are labeled to the right of the panel. (b) Transfer reactions with all four donor constructs in the presence of the initial acceptor (A0) were performed. Transfer efficiency after 30 min is depicted as the total of transfers before the marker (hatched bar) and transfers after the marker (black bar). The total transfer efficiency is given above each bar, and the percentage of total transfers that occur before the marker is shown to the right of each bar. Results represent the average of at least three experiments. (c) Reactions were performed as described for (b) in the presence of 50% NC coating (100% = 1 NC per 7 nt). NC was incubated with the template for 5 min prior to the addition of RT. (d) Reactions were performed as described for (b), except the acceptor template with the corresponding mutations was used with each donor.

invasion, and the distribution of transfers all remaining unchanged from that observed with A0 (compare Figure 8(b) and (d)). These results support the conclusion that acceptor structure can influence the mechanism and ultimate position of transfers.

Acceptor cleavage confirms the same invasion site for A0 and A1

In order to confirm the putative invasion site defined by the blocking oligomer and RNase H digestion data, we followed degradation of the acceptor template during a transfer reaction. These experiments were performed in the presence of 50% NC coating with a 5′ end-labeled acceptor template. Interactions between the cDNA and acceptor would produce a hybrid allowing for RT RNase H cleavage of the acceptor template in these regions. Interactions leading to cleavages early in a time-course would likely correspond to the initial invasion site.[73] Consistent with this, RT was able to cleave both A0 and A1 between 100 nt and 120 nt at the putative invasion site within one minute (Figure 9). After two and four minutes there were also substantial amounts of cleavage at the end of the homology between the donor and acceptor (50–65 nt) and the end of the full-length transfer products (0–20 nt), respectively. It is also significant

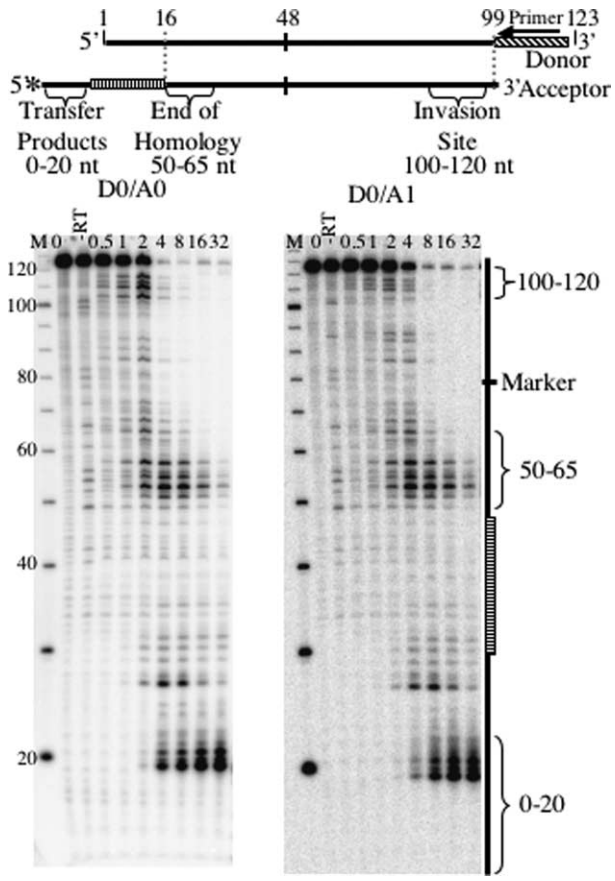

Figure 9. Acceptor cleavage during a transfer reaction. Acceptor RNA with a (5′-^{32}P) end label was followed during transfer reactions performed at a 1:1 ratio of donor/acceptor, with 64 nM RT, and 50% NC coating (100% = 1 NC/7 nt). Reactions were stopped at 0.5, 1, 2, 4, 8, 16, and 32 min, and separated on a 10% polyacrylamide gel. A 10 bp ladder (M) was run on each panel and is labeled to the left. A representation of the acceptor template, with a hatched bar representing the unique region, is shown on the right along with regions of cleavage. A diagram of the expected intermediate leading to cleavage in each region is shown.

that 14% of the total counts in the lane at 2 min were located within the putative invasion region (100–120 nt; Figure 9) with A0 but only 8% with A1. A similar cleavage pattern was seen when D1 was used with A0 and A1 (data not shown), suggesting that both donor templates use the same major invasion site with both acceptors. We interpret this to mean that A1 is less efficient at invasion in this region, resulting in the formation of less cleavable hybrid.

Discussion

We previously proposed that the transfer process involves the sequential steps of donor cleavage, acceptor invasion, hybrid propagation, and primer terminus switch.[50] Analysis of strand transfer *in vitro* using a variety of template systems, including HIV-1 minus strong stop transfer, showed that invasion and primer terminus transfer are distinct and spatially separated.[38,41,50] In this work, we designed RNA templates to specifically address the role of RT pausing and template structure on the acceptor invasion and primer terminus transfer steps of the transfer process.

Our original thoughts in designing this system were that introduction of a stable structure in the donor template would produce a pause site with associated RNase H cleavage that would then lead to acceptor invasion and increased transfer. Strengthening secondary structures produced the expected pause sites and associated RNase H cleavage on the donor template. Also as expected, increased pausing on the donor template increased the transfer efficiency (Figures 3 and 8(b)). However, the effectiveness of pause sites at increasing transfer varied with different templates. With acceptor A0, transfer efficiency with donor D1 was four times that of D0, while the transfer efficiencies of D2 and D3 were only twice that of D0. We also observed that donor cleavages associated with the newly introduced pause sites did not always produce the expected increase in invasion when assessed by blocking oligomers. Extensive RNase H cleavage in a specific region of the donor template coupled with effective inhibition of transfer by a blocking oligomer corresponding to that region would be indicative of an effective acceptor invasion site. Interestingly, in each of the four donor templates, weak pause sites were sufficient to direct RNase H cleavages to create an effective invasion site (75–98 nt region; Figure 4). Blocking oligomer B effectively inhibited transfers in all cases except D1–A0, by 50% (Figure 5). Clearly, the mere presence of a pause site and concomitant RNase H cleavage of the donor were not the complete determinants of transfer efficiency. The combined data from donor cleavage profiles and blocking oligomer analysis support the arguments that (1) weak pause sites can promote sufficient RNase H cuts to create an effective invasion site, and (2) not all pause sites, irrespective of intensity, promote invasion and transfer.

Characteristics of transfers with the various donor and acceptor templates used here suggest that factors in addition to RT pausing and pause-associated donor cleavage are involved in facilitating transfer. Work from several groups has suggested that acceptor structure can influence the transfer reaction.[49,50,74–76] Our data support the conclusion that the acceptor invasion step of the transfer process requires a favorable combination of donor cleavage and acceptor structure. This was best observed with the D1 and D0 associated transfers. For the D0–A0 template pair, blocking oligomers in combination with donor cleavage analysis identified a primary region of acceptor invasion at the donor 3′ end (77–98 nt region). When D1, which had increased pause-associated cleavage within this region, was used as

the donor, transfer efficiency increased to four times that of D0. The cleavages on D1 very likely allowed for efficient acceptor invasion by A0 as compared to the cleavages on D0. Changing the acceptor from A0 to A1 decreased transfer efficiency for both D0 and D1 by half. Structural analysis using RNase T_1 digestion and Mfold analysis predicted the 3′ terminal 38 nt of the acceptor RNA A0 to have weak secondary structure, while A1 had a much more stable secondary structure in this region (Figure 6(b) and (c)). We interpret this to mean that the stabilized structure in the 3′ region of A1 made invasion less efficient at the donor cleavage site on D1 and D0, resulting in lower efficiency of transfers with A1 as compared to A0. Consistent with this interpretation, acceptor cleavage showed a higher proportion of cleavages in this region for A0 than A1 (Figure 9). Additionally, transfers promoted by D2 and D3, which also involved the same primary invasion site, were less efficient with A1 compared to A0 (Figure 7). In conclusion, although RNase H cleavages (associated with strong or weak pause sites) in each of the four donor templates created potential invasion sites, the structure of the acceptor very likely dictated whether the exposed region was utilized for invasion and transfer. The data thus suggest that donor cleavages in combination with the acceptor structure promote acceptor–cDNA interaction and transfer.

Our expectation, based on a previous study of pause-induced transfers, was that the primer terminus switch would occur at a distance from the pause site. Contrary to this expectation, while both D1 and D2 promoted more transfers than D0, the large majority occurred before the marker (84–86%; Figure 8(b)), in close proximity to the pause site. Using the corresponding mutant acceptor A2 with sequence identical with that of the mutant donor D2, which had the least homology with A0, did not alter transfer efficiency or distribution, suggesting a partial lack of local homology between the initial template pair was not the cause of the short distance transfers. Characteristics of the transfer were clearly different in these templates as compared to pause-induced two-step transfers previously analyzed in stable hairpin templates.[44,46,50,51] It is possible that transfers in D1 and D2 occurred by a primer terminus switch mechanism not involving an acceptor invasion process. Here pause-associated donor cleavage would free the primer terminus, enabling it to anneal to the acceptor. Alternately, transfer still occurred by the two-step mechanism in D1 and D2, but with the acceptor invasion and primer terminus transfer steps occurring within a relatively short distance of each other before the marker. Since both templates still used the 3′ region of weak pausing for invasion (77–98 nt region; Figure 5) a likely effect of the newly introduced pause sites in D1 and D2 may have been a stalling of synthesis, thereby allowing invasion to catch up with the primer terminus completing transfers at these pause sites before the marker. This mechanism is consistent with the idea that pausing after the invasion site allows the expanding hybrid to catch the extending primer terminus.[40,50,77] For D1 and D3, changing the acceptor from A0 to A1 or A3, respectively, had a modest effect on transfer distribution, indicating that acceptor structure can also influence the primer terminus transfer step. Derebail & DeStefano also showed that increasing acceptor structure can shift transfers towards the 5′ end of the template, presumably by decreasing the rate of hybrid propagation.[40] While we have gained an understanding of some of the factors that promote acceptor invasion, the precise factors and mechanism that promote the terminus transfer step remains poorly understood. Hybrid propagation and terminus transfer steps are topics of a current investigation in our laboratory.

Combining donor cleavage, blocking oligomer inhibition, acceptor cleavage, and transfer distribution reveals characteristics of transfers on the various donor–acceptor templates. In the case of D1, the P1 pause site increased donor cleavage in the favored region of acceptor invasion, accounting for the increased transfer efficiency with D1–A0. Also, the majority of transfers on D1–A0 were completed before the marker. One discrepancy, however, is that although 84% of transfers occurred before the marker, oligomer B caused only a 30% inhibition of transfer. Since acceptor cleavage suggests that this is the major region of invasion for this template pair (data not shown), it is possible that DNA oligomers are less effective at competing with the RNA acceptor at sites where invasion is very efficient. The less efficient transfers with the structured A1 were more sensitive to oligomer B (50% with A1 *versus* 30% with A0).

Also oligomer G could be inhibiting either acceptor–cDNA interactions that initiate in the 5′ region on the template, or the primer terminus switch for acceptors that invaded earlier on the cDNA. The slight increase in efficiency of oligomers G and H with A1 *versus* A0 on D1 is likely related to both the small increase in transfers after the marker and other uncharacterized effects.

With donor D2–A0, there is an increase in transfer efficiency to 7% (from 3.5% for D0), with 86% of transfers occurring before the marker. D2 shows extensive cleavages in the 60–100 nt region (Figure 4). This opens up a wide area of the cDNA for acceptor invasion and transfer. Increased effectiveness of oligomer B *versus* oligomer D in inhibiting transfer is not surprising, as the most concentrated region of cleavage overlaps predominantly with oligomer B, in a region of the acceptor that is predicted to be weakly structured. In the case of donor D3, increased cleavage is seen in the 50–70 nt region (Figure 4), immediately adjacent to the marker, with blocking oligomers D and B inhibiting transfers equally (40–45%). However, with acceptor A3, oligomer D showed the most inhibition (55%; Figure 5(e)). Mfold predictions indicated A3 to be less structured in the region corresponding to oligomer D. This again suggests a role for acceptor

structure in determining the utilization of invasion sites.

NC increases donor cleavage[41,46,66,72] and improves the interaction between cDNA and acceptor templates.[39,48,63–65] Such effects of NC could contribute to the increased *TE* value observed with all of the templates. In the case of D0 and D3, NC also caused an increase in transfers completed before the marker. A similar effect of NC has also been observed for transfers with other template systems.[38] This shift in transfers could result from one of two mechanisms. NC-induced donor cleavage and invasion promoted more efficient terminus transfers at the invasion site. Alternately, NC promoted efficient hybrid propagation,[61] thereby reducing the separation of the invasion and terminus transfer in two-step transfers.

Accumulating evidence from mechanistic studies shows that the transfer mechanism involves additional factors beyond the currently understood concept that pausing produces RNase H cleavages that promote template switching. Our conclusions from this study support the involvement of template structure and show that: (1) all prominent pause sites did not necessarily create an effective invasion site; (2) the most effective invasion site in our system was generated from template cleavages associated with weak pauses even in the presence of nearby strong pauses; (3) acceptor invasion and transfer appeared to require both a region of donor cleavages, and a favorable acceptor structure for strand interaction in this region; (4) transfer distributions indicated that the acceptor structure also influences the primer terminus transfer step.

Materials and Methods

Reagents

Recombinant heterodimer HIV-1 reverse transcriptase was purified as described.[46,78] Chemically synthesized nucleocapsid protein (1–72) NCp7 was generously provided by Dr Bernard P. Roques.[79] NC was stored at −80 °C in a buffer of 50 mM Tris–HCl (pH 7.5), 5 mM dithiothreitol. DH5α competent cells and Taq polymerase were from Invitrogen (San Diego, CA). Radiolabeled compounds were from Perkin–Elmer Life Sciences (Boston, MA), and Micro Bio-Spin columns were from Bio-Rad (Hercules, CA). Integrated DNA Technologies, Inc. (Coralville, IA) synthesized all DNA primers. The pBluescript II KS (+) plasmid was obtained from Stratagene (La Jolla, CA). All other enzymes were purchased from Roche Molecular Biochemicals (Indianapolis, IN).

Generation of donor and acceptor templates

D0 was made by annealing primers Don1 and Don2 and extending with Taq polymerase (Don1, 5′-CAGACTGGGCCCTCACTACACATCGCAGTACAAGTCTAAGCTTACATCAGATCGATGACTCAAGAATGTTTACC; Don2, 5′-TCTAGGATCCGACGCATGTGACTG-ATATCCGGTTCTATAACGGTATGATGGTAAACATTCTTGAGTCATCG: underlined regions correspond to complementary sequences). A0 was made the same way using primers Acc1 and Acc2 (Acc1, 5′-CAGACTGGGCCCCGATCCTACGAGT-ATACGTCTCACTACACATCGCAGTACAAGTCTAAGCTAACATCAGAT; Acc2, 5′-TCTAGGATCCGGTTCTATAACGGTATGATGGTAAACATTCTTGAGTCATCG-ATCTGATGTTAGCTTAGACT; underlined regions correspond to complementary sequences). Donor products were PCR amplified using the primers MH27, 5′-AGTCAGGAGCTCCTCACTACACATCGCAGTACAAGTC; and MH28, 5′- CTGTC-AGGATCCGACGCATGTGACTGATATCCGGTTC; while acceptor products were PCR amplified using the primers MH29, 5′-AGTCAGGAGCTCCGATCCTACGAG-TATACGTCTCAC; and MH30, 5′-CTGTCAGGATCCCGGTTCTATAACGGTATG-ATGG; and both were cloned into the SacI and BamHI sites of pBluescript II KS (+), creating D0 and A0 plasmids. The various mutations to create D1, D2, D3, A1, A2, and A3 templates were introduced into these plasmids using an overlap PCR approach as described.[80] The internal overlap primers with the mutations were as follows: for D1, and A1 (MH51 (+), 5′-CAAGAATGTTTGCCCTC-ATACCG; MH54 (−), 5′-CGGTATGAGGGCAAACATTCTTG); for D2 (MH52 (+), 5′-GCTTACCCGAGATCCGGGACTCAAG; MH55 (−), 5′-CTTGAGTCCCGGATCT-CGGGTAAGC); for A2 (MH52A (+), 5′-GCTAACCCGAGATCCGGGACTCAAG; MH55A (−), 5′-CTTGAGTCCCGGATCTCGGGTTAGC); for D3 (MH53 (+), 5′-GGAGCTCCTGACTTGACATCGC; MH56 (−), 5′-GCGATGTCAAGTCAGGAGC-TCC); and for A3 (MH53A (+), 5′-GTATACGTCTGACTTGACATCGC; MH56A (−), 5′-GCGATGTCAAGTCAGACGTATAC). Introduced mutations are underlined. These overlap primers were used with the outer primers (MH49, 5′-CTGCAAGGCGATTAA-GTTGG and MH50, 5′-GATATCGAATTCCTGCAGCC, or MH47, 5′-GGTTTTCCCA-GTCACGACG and MH48, 5′-GGAACAAAAGCTGGGTACCG) to generate PCR fragments which were digested with SacI and BamHI, and cloned back into pBluescript II KS (+). Constructs were transformed into *Escherichia coli* DH5α cells and sequenced.

RNA templates were generated *in vitro* by run-off transcription from BamHI-linearized plasmids using T7 RNA polymerase, as described in the manufacturer's protocol (Roche Molecular Biochemicals). RNA substrates were gel-purified.

Labeling and annealing of substrates

DNA primers or RNA templates (RNA templates first treated with calf intestine phosphatase) were labeled at the 5′ end using polynucleotide kinase and [γ-^{32}P]ATP (6000 Ci/mmol). Unincorporated nucleotides were separated using P-30 Micro Bio-Spin columns (Bio-Rad). Donor RNA (either labeled or unlabeled), acceptor RNA, and primer (either labeled or unlabeled) at a ratio of 1:2:1.5 were brought to a volume of 10 μl in 50 mM Tris–HCl (pH 8.0), 80 mM KCl, 1 mM dithiothreitol, and 1 mM EDTA, heated for 5 min at 95 °C, and slow-cooled to room temperature. All the donors were primed with the same primer MH21 (5′-GACGCATGTGACTGATATCC) and acceptor extension assays were performed using MH65 (5′-ATCCGGTTCTATAACGGTATG) as the primer.

Reverse transcriptase assays

Reactions were carried out in a final volume of 12.5 μl. For extension reactions 32 nM of HIV-1 reverse

transcriptase were incubated for 5 min at room temperature with 4 nM annealed template-primer termini (see above) in 50 mM Tris–HCl (pH 8), 80 mM KCl, 1 mM dithiothreitol, and 1 mM EDTA. Reactions were started by adding dNTPs and $MgCl_2$ to a final concentration of 50 μM and 6 mM, respectively. Acceptor RNA (8nM) was included for strand transfer assays. Transfer assays were performed with 5′ end-labeled primer, while RNase H assays were performed with 5′end-labeled donor RNA. Reactions were incubated at 37 °C and stopped at the appropriate time by adding 1 volume of 2× termination buffer (90% (v/v) formamide, 10 mM EDTA (pH 8), and 0.1% (w/v) each of bromophenol blue and xylene cyanol). For reactions with blocking oligonucleotides, 15 nM of oligonucleotide was added at the same time as the dNTPs and $MgCl_2$. Blocking oligonucleotides used were B (5′-ACCATCATACCGTTATAGAACC), C (5′-GACTCA AGAATGTTTACCATC), D (5′-TCGATGACTCAAGAA TGTTTACC), E (5′-AGTCTAAGCTTACATCAGATCG), F (5′- ACATCGCAGTACAAGTCTAAGCT), G (5′-CT CACTACACATCGCAGTA-CAAGTCTAAG), H (5′-CTC ACACACATCGCAGT), Ctrl (5′-GAATCTGAACATGA-CGCTACACATCACTC), underlined sequences were changed as needed to maintain 100% complementarity with the various cDNAs produced. Reaction products were resolved on a urea/8% (w/v) polyacrylamide gel, and visualized using a PhosphorImager and ImageQuant software (Amersham Biosciences). Transfer efficiency (TE) was determined using the formula TE = (TP/(FL + TP)), where FL is full length extension of the donor, and TP is full length extension of transfer products on the acceptor.

Acceptor cleavage

Reactions conditions were similar to those in transfer reactions described above with slight modification. NC was added to template-primer-acceptor at a 50% coating level (100% = 1 NC/7 nt) and incubated for 5 min at 37 °C. Then 64 nM HIV-1 RT was pre-bound to the substrate for 2 min at 37 °C before dNTPs and $MgCl_2$ were added to initiate the reaction. Final conditions were 4 nM annealed template-primer termini (see above), 4 nM 5′ end-labeled acceptor, 50 mM Tris–HCl (pH 8), 80 mM KCl, 1 mM dithiothreitol, 1 mM EDTA, 17 μM dNTPs and 6 mM $MgCl_2$. Reactions were stopped at various times by adding an equal volume of 2× termination buffer (see above). Samples were then separated on a urea/10% polyacrylamide gel, and visualized using a PhosphorImager and ImageQuant software.

Analysis of transfer products

To determine the transfer distribution, transfer products were isolated from an 8% polyacrylamide gel and amplified using a protocol modified from Jo *et al*.[81] Excised gel fragments were soaked in 300 μl of distilled water for 10 min. The tubes were then boiled for 15 min, and sedimented at 10,000*g* for 2 min. Extracted DNA was ethanol-precipitated. The recovered DNA pellet was washed with cold 85% ethanol and dissolved in 12 μl of distilled water.

Four microliters of the extracted DNA was used in a 40 μl PCR. Final reaction components were 20 mM Tris–HCl (pH 8.4), 50 mM KCl, 1.5 mM $MgCl_2$, 0.4 mM dNTPs, 2 μM each primer MH31 (5′-CCGATCCTACGAGTA TACG), and 5′ end-labeled MH21 (see above), and two units of Taq polymerase (Invitrogen). Reactions were heated at 95 °C for 2 min, and PCR amplification was performed for 25 cycles at 95 °C for 2 min, 60 °C for 1 min, 72 °C for 1 min followed by extension for 10 min at 72 °C. The PCR products were then digested with either AluI or HindIII for 1 h at 37 °C. The digested products were separated on a urea/10% polyacrylamide gel, and visualized as described above. External primers used for the PCR control reactions were MH31 and MH21, the internal primers were MH23 (5′-CTCACTACACATCG CAGTAC) and MH65 (5′-ATCCGGTTCTATAACGGT ATG). PCR products were handled as described above, and the ratio ((% FL external primers/% FL internal primers)×100) defined the maximum recombination rate for PCR amplification.

RNase T_1 digestion

The 20 nM 5′end-labeled acceptor template was heated to 95 °C and cooled to room temperature in 50 mM Tris–HCl (pH 8), 80 mM KCl, 1 mM dithiothreitol, 1.65 μM yeast tRNA, and 1 mM EDTA. Reactions were started by adding $MgCl_2$ to 6 mM and 0.2 unit of RNase T_1. They were stopped at the appropriate time by adding one volume of stop mix (30 mM EDTA (pH 8), 0.6 M sodium acetate) and placing on ice. Products were ethanol-precipitated, separated on a urea/10% polyacrylamide gel, and visualized as described above.

Acknowledgements

We thank Dr Vandana Purohit for helpful discussions and critical reading of the manuscript, along with Dr Ricardo Roda for helpful discussions. This work was supported by National Institute of Health grant GM 049573 to R.A.B., and M.N.H. was funded by National Institute of Health Training grant T32-CA09363.

References

1. Telesnitsky, A. & Goff, S. P. (1993). Strong-stop strand transfer during reverse transcription.In *Reverse Transcriptase* (Skalka, A. M., & Goff, S. P., eds), pp. 49–83, Cold Spring Harbor Laboratory Press, Cold Spring Harbor, NY.
2. Brown, P. O. (1997). Integration. In *Retroviruses* (Coffin, J. M., Hughes, S. H. & Varmus, H., eds), pp. 161–204, Cold Spring Harbor Laboratory Press, Cold Spring Harbor, NY.
3. Telesnitsky, A. & Goff, S. P. (1997). Reverse transcriptase and the generation of retroviral DNA. In *Retroviruses* (Coffin, J. M., Hughes, S. H. & Varmus, H. E., eds), pp. 121–160, Cold Spring Harbor Laboratory Press, Cold Spring Harbor, NY.
4. Clavel, F., Hoggan, M. D., Willey, R. L., Strebel, K., Martin, M. A. & Repaske, R. (1989). Genetic recombination of human immunodeficiency virus. *J. Virol.* **63**, 1455–1459.
5. Goodrich, D. W. & Duesberg, P. H. (1990). Retroviral recombination during reverse transcription. *Proc. Natl Acad. Sci. USA*, **87**, 2052–2056.
6. Hu, W. S. & Temin, H. M. (1990). Genetic consequences of packaging two RNA genomes in one

retroviral particle: pseudodiploidy and high rate of genetic recombination. *Proc. Natl Acad. Sci. USA*, **87**, 1556–1560.
7. Jetzt, A. E., Yu, H., Klarmann, G. J., Ron, Y., Preston, B. D. & Dougherty, J. P. (2000). High rate of recombination throughout the human immunodeficiency virus type 1 genome. *J. Virol.* **74**, 1234–1240.
8. Zhuang, J., Jetzt, A. E., Sun, G., Yu, H., Klarmann, G., Ron, Y. *et al*. (2002). Human immunodeficiency virus type 1 recombination: rate, fidelity, and putative hot spots. *J. Virol.* **76**, 11273–11282.
9. Rhodes, T., Wargo, H. & Hu, W.-S. (2003). High rates of human immunodeficiency virus type 1 recombination: near-random segregation of markers one kilobase apart in one round of viral replication. *J. Virol.* **77**, 11193–11200.
10. Pekrun, K., Shibata, R., Igarashi, T., Reed, M., Sheppard, L., Patten, P. A. *et al*. (2002). Evolution of a human immunodeficiency virus type 1 variant with enhanced replication in pig-tailed macaque cells by DNA shuffling. *J. Virol.* **76**, 2924–2935.
11. Robertson, D. L., Hahn, B. H. & Sharp, P. M. (1995). Recombination in AIDS viruses. *J. Mol. Evol.* **40**, 249–259.
12. Gu, Z., Gao, Q., Faust, E. A. & Wainberg, M. A. (1995). Possible involvement of cell fusion and viral recombination in generation of human immunodeficiency virus variants that display dual resistance to AZT and 3TC. *J. Gen. Virol.* **76**, 2601–2605.
13. Gunthard, H. F., Leigh-Brown, A. J., D'Aquila, R. T., Johnson, V. A., Kuritzkes, D. R., Richman, D. D. *et al*. (1999). Higher selection pressure from antiretroviral drugs *in vivo* results in increased evolutionary distance in HIV-1 pol. *Virology*, **259**, 154–165.
14. Kellam, P. & Larder, B. A. (1995). Retroviral recombination can lead to linkage of reverse transcriptase mutations that confer increased zidovudine resistance. *J. Virol.* **69**, 669–674.
15. Boyer, J. C., Bebenek, K. & Kunkel, T. A. (1992). Unequal human immunodeficiency virus type 1 reverse transcriptase error rates with RNA and DNA templates. *Proc. Natl Acad. Sci. USA*, **89**, 6919–6923.
16. Ji, J. P. & Loeb, L. A. (1992). Fidelity of HIV-1 reverse transcriptase copying RNA *in vitro*. *Biochemistry*, **31**, 954–958.
17. Preston, B. D., Poiesz, B. J. & Loeb, L. A. (1988). Fidelity of HIV-1 reverse transcriptase. *Science*, **242**, 1168–1171.
18. Roberts, J. D., Bebenek, K. & Kunkel, T. A. (1988). The accuracy of reverse transcriptase from HIV-1. *Science*, **242**, 1171–1173.
19. Weber, J. & Grosse, F. (1989). Fidelity of human immunodeficiency virus type I reverse transcriptase in copying natural DNA. *Nucl. Acids Res.* **17**, 1379–1393.
20. Anderson, J. A., Teufel, R. J., 2nd, Yin, P. D. & Hu, W. S. (1998). Correlated template-switching events during minus-strand DNA synthesis: a mechanism for high negative interference during retroviral recombination. *J. Virol.* **72**, 1186–1194.
21. Hu, W. S. & Temin, H. M. (1992). Effect of gamma radiation on retroviral recombination. *J. Virol.* **66**, 4457–4463.
22. Zhang, J., Tang, L.-Y., Li, T., Ma, Y. & Sapp, C. M. (2000). Most retroviral recombinations occur during minus-strand DNA synthesis. *J. Virol.* **74**, 2313–2322.
23. Xu, H. & Boeke, J. D. (1987). High-frequency deletion between homologous sequences during retrotransposition of Ty elements in *Saccharomyces cerevisiae*. *Proc. Natl Acad. Sci. USA*, **84**, 8553–8557.
24. Blain, S. W. & Goff, S. P. (1995). Effects on DNA synthesis and translocation caused by mutations in the RNase H domain of Moloney murine leukemia virus reverse transcriptase. *J. Virol.* **69**, 4440–4452.
25. Brincat, J. L., Pfeiffer, J. K. & Telesnitsky, A. (2002). RNase H activity is required for high-frequency repeat deletion during Moloney murine leukemia virus replication. *J. Virol.* **76**, 88–95.
26. Cameron, C. E., Ghosh, M., Le Grice, S. F. J. & Benkovic, S. J. (1997). Mutations in HIV reverse transcriptase which alter RNase H activity and decrease strand transfer efficiency are suppressed by HIV nucleocapsid protein. *Proc. Natl Acad. Sci. USA*, **94**, 6700–6705.
27. DeStefano, J. J., Mallaber, L. M., Rodriguez-Rodriguez, L., Fay, P. J. & Bambara, R. A. (1992). Requirements for strand transfer between internal regions of heteropolymer templates by human immunodeficiency virus reverse transcriptase. *J. Virol.* **66**, 6370–6378.
28. Gabbara, S., Davis, W. R., Hupe, D. & Peliska, J. A. (1999). Inhibitors of DNA strand transfer reactions catalyzed by HIV-1 reverse transcriptase. *Biochemistry*, **38**, 13070–13076.
29. Hu, W. S., Pathak, V. K. & Temin, H. M. (1993). Role of reverse transcriptase in retroviral recombination. In *Reverse Transcriptase* (Skalka, A. M. & Goff, S. P., eds), pp. 251–274, Cold Spring Harbor Laboratory Press, Cold Spring Harbor, NY.
30. Peliska, J. A. & Benkovic, S. J. (1992). Mechanism of DNA strand transfer reactions catalyzed by HIV-1 reverse transcriptase. *Science*, **258**, 1112–1118.
31. Svarovskaia, E. S., Delviks, K. A., Hwang, C. K. & Pathak, V. K. (2000). Structural determinants of murine leukemia virus reverse transcriptase that affect the frequency of template switching. *J. Virol.* **74**, 7171–7178.
32. An, W. & Telesnitsky, A. (2002). Effects of varying sequence similarity on the frequency of repeat deletion during reverse transcription of a human immunodeficiency virus type 1 vector. *J. Virol.* **76**, 7897–7902.
33. Colicelli, J. & Goff, S. P. (1987). Identification of endogenous retroviral sequences as potential donors for recombinational repair of mutant retroviruses: positions of crossover points. *Virology*, **160**, 518–522.
34. Dang, Q. & Hu, W. S. (2001). Effects of homology length in the repeat region on minus-strand DNA transfer and retroviral replication. *J. Virol.* **75**, 809–820.
35. Pfeiffer, J. K. & Telesnitsky, A. (2001). Effects of limiting homology at the site of intermolecular recombinogenic template switching during moloney murine leukemia virus replication. *J. Virol.* **75**, 11263–11274.
36. Ohi, Y. & Clever, J. L. (2000). Sequences in the 5′ and 3′ R elements of human immunodeficiency virus type 1 critical for efficient reverse transcription. *J. Virol.* **74**, 8324–8334.
37. Yin, P. D., Pathak, V. K., Rowan, A. E., Teufel, R. J., 2nd & Hu, W. S. (1997). Utilization of nonhomologous minus-strand DNA transfer to generate recombinant retroviruses. *J. Virol.* **71**, 2487–2494.
38. Balakrishnan, M., Roques, B. P., Fay, P. J. & Bambara, R. A. (2003). Template dimerization promotes an

acceptor invasion-induced transfer mechanism during human immunodeficiency virus type 1 minus-strand synthesis. *J. Virol.* **77**, 4710–4721.
39. Derebail, S. S., Heath, M. J. & DeStefano, J. J. (2003). Evidence for the differential effects of nucleocapsid protein on strand transfer in various regions of the HIV genome. *J. Biol. Chem.* **278**, 15702–15712.
40. Derebail, S. S. & DeStefano, J. J. (2004). Mechanistic analysis of pause site-dependent and -independent recombinogenic strand transfer from structurally diverse regions of the HIV genome. *J. Biol. Chem.* **279**, 47446–47454.
41. Chen, Y., Balakrishnan, M., Roques, B. P. & Bambara, R. A. (2003). Steps of the acceptor invasion mechanism for HIV-1 minus strand strong stop transfer. *J. Biol. Chem.* **278**, 8006–8017.
42. Diaz, L. & DeStefano, J. J. (1996). Strand transfer is enhanced by mismatched nucleotides at the 3′ primer terminus: a possible link between HIV reverse transcriptase fidelity and recombination. *Nucl. Acids Res.* **24**, 3086–3092.
43. Harrison, G. P., Mayo, M. S., Hunter, E. & Lever, A. M. (1998). Pausing of reverse transcriptase on retroviral RNA templates is influenced by secondary structures both 5′ and 3′ of the catalytic site. *Nucl. Acids Res.* **26**, 3433–3442.
44. Kim, J. K., Palaniappan, C., Wu, W., Fay, P. J. & Bambara, R. A. (1997). Evidence for a unique mechanism of strand transfer from the transactivation response region of HIV-1. *J. Biol. Chem.* **272**, 16769–16777.
45. Palaniappan, C., Fuentes, G. M., Rodriguez-Rodriguez, L., Fay, P. J. & Bambara, R. A. (1996). Helix structure and ends of RNA/DNA hybrids direct the cleavage specificity of HIV-1 reverse transcriptase RNase H. *J. Biol. Chem.* **271**, 2063–2070.
46. Roda, R. H., Balakrishnan, M., Hanson, M. N., Wohrl, B. M., Le Grice, S. F. J., Roques, B. P. *et al*. (2003). Role of the reverse transcriptase, nucleocapsid protein, and template structure in the two-step transfer mechanism in retroviral recombination. *J. Biol. Chem.* **278**, 31536–31546.
47. Wu, W., Blumberg, B. M., Fay, P. J. & Bambara, R. A. (1995). Strand transfer mediated by human immunodeficiency virus reverse transcriptase *in vitro* is promoted by pausing and results in misincorporation. *J. Biol. Chem.* **270**, 325–332.
48. Negroni, M. & Buc, H. (1999). Recombination during reverse transcription: an evaluation of the role of the nucleocapsid protein. *J. Mol. Biol.* **286**, 15–31.
49. Negroni, M. & Buc, H. (2000). Copy-choice recombination by reverse transcriptases: reshuffling of genetic markers mediated by RNA chaperones. *Proc. Natl Acad. Sci. USA*, **97**, 6385–6390.
50. Roda, R. H., Balakrishnan, M., Kim, J. K., Roques, B. P., Fay, P. J. & Bambara, R. A. (2002). Strand transfer occurs in retroviruses by a pause-initiated two-step mechanism. *J. Biol. Chem.* **277**, 46900–46911.
51. Chen, Y., Balakrishnan, M., Roques, B. P., Fay, P. J. & Bambara, R. A. (2003). Mechanism of minus strand strong stop transfer in HIV-1 reverse transcription. *J. Biol. Chem.* **278**, 8006–8017.
52. Darlix, J. L., Lapadat-Tapolsky, M., de Rocquigny, H. & Roques, B. P. (1995). First glimpses at structure–function relationships of the nucleocapsid protein of retroviruses. *J. Mol. Biol.* **254**, 523–537.
53. Rein, A., Henderson, L. E. & Levin, J. G. (1998). Nucleic-acid-chaperone activity of retroviral nucleocapsid proteins: significance for viral replication. *Trends Biochem. Sci.* **23**, 297–301.
54. Allain, B., Lapadat-Tapolsky, M., Berlioz, C. & Darlix, J. L. (1994). Transactivation of the minus-strand DNA transfer by nucleocapsid protein during reverse transcription of the retroviral genome. *EMBO J.* **13**, 973–981.
55. Darlix, J. L., Vincent, A., Gabus, C., de Rocquigny, H. & Roques, B. (1993). Trans-activation of the 5′ to 3′ viral DNA strand transfer by nucleocapsid protein during reverse transcription of HIV1 RNA. *C.R. Acad. Sci. III*, **316**, 763–771.
56. Rodriguez-Rodriguez, L., Tsuchihashi, Z., Fuentes, G. M., Bambara, R. A. & Fay, P. J. (1995). Influence of human immunodeficiency virus nucleocapsid protein on synthesis and strand transfer by the reverse transcriptase *in vitro*. *J. Biol. Chem.* **270**, 15005–15011.
57. DeStefano, J. J. (1996). Interaction of human immunodeficiency virus nucleocapsid protein with a structure mimicking a replication intermediate. Effects on stability, reverse transcriptase binding, and strand transfer. *J. Biol. Chem.* **271**, 16350–16356.
58. Golinelli, M. P. & Hughes, S. H. (2003). Secondary structure in the nucleic acid affects the rate of HIV-1 nucleocapsid-mediated strand annealing. *Biochemistry*, **42**, 8153–8162.
59. Hsu, M., Rong, L., de Rocquigny, H., Roques, B. P. & Wainberg, M. A. (2000). The effect of mutations in the HIV-1 nucleocapsid protein on strand transfer in cell-free reverse transcription reactions. *Nucl. Acids Res.* **28**, 1724–1729.
60. Lapadat-Tapolsky, M., Pernelle, C., Borie, C. & Darlix, J. L. (1995). Analysis of the nucleic acid annealing activities of nucleocapsid protein from HIV-1. *Nucl. Acids Res.* **23**, 2434–2441.
61. Tsuchihashi, Z. & Brown, P. O. (1994). DNA strand exchange and selective DNA annealing promoted by the human immunodeficiency virus type 1 nucleocapsid protein. *J. Virol.* **68**, 5863–5870.
62. You, J. C. & McHenry, C. S. (1994). Human immunodeficiency virus nucleocapsid protein accelerates strand transfer of the terminally redundant sequences involved in reverse transcription. *J. Biol. Chem.* **269**, 31491–31495.
63. Raja, A. & DeStefano, J. J. (1999). Kinetic analysis of the effect of HIV nucleocapsid protein (NCp) on internal strand transfer reactions. *Biochemistry*, **38**, 5178–5184.
64. Guo, J., Wu, T., Kane, B. F., Johnson, D. G., Henderson, L. E., Gorelick, R. J. & Levin, J. G. (2002). Subtle alterations of the native zinc finger structures have dramatic effects on the nucleic acid chaperone activity of human immunodeficiency virus type 1 nucleocapsid protein. *J. Virol.* **76**, 4370–4378.
65. Heilman-Miller, S. L., Wu, T. & Levin, J. G. (2004). Alteration of nucleic acid structure and stability modulates the efficiency of minus-strand transfer mediated by the HIV-1 nucleocapsid protein. *J. Biol. Chem.* **279**, 44154–44165.
66. Peliska, J. A., Balasubramanian, S., Giedroc, D. P. & Benkovic, S. J. (1994). Recombinant HIV-1 nucleocapsid protein accelerates HIV-1 reverse transcriptase catalyzed DNA strand transfer reactions and modulates RNase H activity. *Biochemistry*, **33**, 13817–13823.
67. Zuker, M. (2003). Mfold web server for nucleic acid folding and hybridization prediction. *Nucl. Acids Res.* **31**, 3406–3415.
68. Suo, Z. & Johnson, K. A. (1997). RNA secondary

structure switching during DNA synthesis catalyzed by HIV-1 reverse transcriptase. *Biochemistry*, **36**, 14778–14785.
69. Suo, Z. & Johnson, K. A. (1997). Effect of RNA secondary structure on RNA cleavage catalyzed by HIV-1 reverse transcriptase. *Biochemistry*, **36**, 12468–12476.
70. DeStefano, J. J., Bambara, R. A. & Fay, P. J. (1994). The mechanism of human immunodeficiency virus reverse transcriptase-catalyzed strand transfer from internal regions of heteropolymeric RNA templates. *J. Biol. Chem.* **269**, 161–168.
71. Guo, J., Wu, T., Anderson, J., Kane, B. F., Johnson, D. G., Gorelick, R. J. *et al*. (2000). Zinc finger structures in the human immunodeficiency virus type 1 nucleocapsid protein facilitate efficient minus- and plus-strand transfer. *J. Virol.* **74**, 8980–8988.
72. Wisniewski, M., Chen, Y., Balakrishnan, M., Palaniappan, C., Roques, B. P., Fay, P. J. & Bambara, R. A. (2002). Substrate requirements for secondary cleavage by HIV-1 reverse transcriptase RNase H. *J. Biol. Chem.* **277**, 28400–28410.
73. Chen, Y., Balakrishnan, M., Roques, B. P. & Bambara, R. A. (2005). Acceptor RNA cleavage profile supports an invasion mechanism for HIV-1 minus strand transfer. *J. Biol. Chem.* **280**, 14443–14452.
74. Berkhout, B., Vastenhouw, N. L., Klasens, B. I. & Huthoff, H. (2001). Structural features in the HIV-1 repeat region facilitate strand transfer during reverse transcription. *RNA*, **7**, 1097–1114.
75. Moumen, A., Polomack, L., Unge, T., Veron, M., Buc, H. & Negroni, M. (2003). Evidence for a mechanism of recombination during reverse transcription dependent on the structure of the acceptor RNA. *J. Biol. Chem.* **278**, 15973–15982.
76. Topping, R., Demoitie, M. A., Shin, N. H. & Telesnitsky, A. (1998). Cis-acting elements required for strong stop acceptor template selection during moloney murine leukemia virus reverse transcription. *J. Mol. Biol.* **281**, 1–15.
77. Lanciault, C. & Champoux, J. J. (2005). Effects of unpaired nucleotides within HIV-1 genomic secondary structures on pausing and strand transfer. *J. Biol. Chem.* **280**, 2413–2423.
78. Pandey, V. N., Kaushik, N., Rege, N., Sarafianos, S. G., Yadav, P. N. & Modak, M. J. (1996). Role of methionine 184 of human immunodeficiency virus type-1 reverse transcriptase in the polymerase function and fidelity of DNA synthesis. *Biochemistry*, **35**, 2168–2179.
79. de Rocquigny, H., Ficheux, D., Gabus, C., Fournie-Zaluski, M. C., Darlix, J. L. & Roques, B. P. (1991). First large scale chemical synthesis of the 72 amino acid HIV-1 nucleocapsid protein NCp7 in an active form. *Biochem. Biophys. Res. Commun.* **180**, 1010–1018.
80. Balakrishnan, M., Fay, P. J. & Bambara, R. A. (2001). The kissing hairpin sequence promotes recombination within the HIV-I 5′ leader region. *J. Biol. Chem.* **276**, 36482–36492.
81. Jo, H., Zhang, H., Zhang, R. & Liang, P. (1998). Cloning oncogenic ras-regulated genes by differential display. *Methods*, **16**, 365–372.

Edited by J. Karn

(Received 13 May 2005; received in revised form 17 August 2005; accepted 26 August 2005)
Available online 26 September 2005